ASIAN JOURNAL OF PHARMACEUTICAL AND CLINICAL RESEARCH

INNOVARE ACADEMIC SCIENCES
Knowledge to Innovation

Vol 18, Issue 4, 2025

Online - 2455-3891
Print - 0974-2441

Research Article

DEVELOPMENT AND EVALUATION OF PRONIOSOMAL GEL FOR ENHANCING THE TRANSDERMAL DELIVERY OF EFINACONAZOLE

VADDURI SWATHI, GADELA V RADHA*

Department of Pharmaceutics, GITAM School of Pharmacy, Visakhapatnam, Andhra Pradesh, India.
***Corresponding author: Gadela V. Radha; Email: rgadela@gitam.edu**

Received: 06 February 2025, Revised and Accepted: 20 March 2025

ABSTRACT

Objectives: The aim of this study was to formulate proniosomes of the antifungal drug efinaconazole to improve its transdermal/topical delivery.

Methods: Proniosomes were prepared using the coacervation phase separation technique. The ideal formulation was selected based on the desirability criterion. Various evaluations were conducted on the optimized formulation, including tests for stability, *ex vivo* permeability, *in vitro* release, skin irritation, surface morphology, and transmission electron microscopy (TEM). The formulation incorporated cholesterol (412.5 mg) and soy lecithin (50 mg), achieving a high encapsulation efficiency. Hydroxypropyl methylcellulose (K4M) was utilized as a polymer in the formulation.

Results: The encapsulation efficiency for cholesterol and soy lecithin reached 82.26%, with the vesicle size measuring 48.32 nm. *In vitro* release studies demonstrated a sustained release of the drug. *Ex vivo* experiments revealed significant differences in the flux of efinaconazole between excised epidermis and membranes. Analysis of surface morphology showed a quick transformation of the proniosomal gel into niosomes. TEM images confirmed the formation of spherical niosomes. The formulations displayed low polydispersity indices (<0.358), indicating uniformity. High zeta potential values prevented flocculation and aggregation, ensuring the stability of the system. Stability testing validated the safety profile of the formulation.

Conclusion: The proniosomal formulation containing efinaconazole exhibited promising potential for enhanced transdermal delivery. The results suggest that this formulation offers improved stability, controlled drug release, and effective permeation, making it a viable candidate for antifungal therapy.

Keywords: Efinaconazole, Proniosomes, Coacervation phase separation, Transdermal delivery, *In vitro* release, *Ex vivo* permeability.

 DOI: http://dx.doi.org/10.22159/ajpcr.2025v18i4.53920. Journal homepage: https://innovareacademics.in/journals/index.php/ajpcr

INTRODUCTION

The transdermal drug delivery system (TDDS) is widely acknowledged as an effective solution to overcome the limitations of the oral route. TDDS enhances the therapeutic efficacy of various drugs by reducing the formation of unwanted metabolites. In addition, it plays a key role in regulating plasma drug levels within living organisms. One of the primary advantages of TDDS is its ability for self-administration and the flexibility to halt medication exposure as needed, resulting in improved patient adherence and minimal variation within and between patients [1]. These innovative drug delivery systems are based on administration methods designed to reduce adverse effects, improve efficacy, decrease toxicity, and offer substantial benefits to patients. The therapeutic index of both existing and novel drug molecules can be improved by encapsulating the active drug within a vesicular structure in one of these systems [2]. A variety of drug delivery systems have been developed, including pharmacosomes, liposomes, niosomes, sphingosomes, ethosomes, and transferosomes. Niosomes and similar vesicular systems have attracted considerable interest in pharmaceutical research as potential vehicles for drug delivery to the skin. These advanced delivery methods have been extensively studied. However, a recurring challenge with niosomal preparations is the occurrence of sedimentation, aggregation, fusion, and vesicle leakage [3]. To address these issues, proniosomes have been developed due to their benefits in transportation, distribution, storage, and dosing. Proniosomes typically appear as dry powder or gel formulations that can convert into niosomes when reconstituted before use. Upon topical application of proniosome gel to the skin within an occlusive environment, the gel hydrates through the skin's moisture and forms niosomes [4]. Proniosomes are capable of encapsulating both lipophilic and hydrophilic molecules. They are mainly composed of a carrier, a membrane stabilizer, and a surfactant, with the ratio of surfactant to other components being adjustable based on the carriers used. Substances such as sorbitol, mannitol, glucose, and lactose enhance the surface area and improve the filling efficiency. This study focuses on incorporating efinaconazole into proniosomes to enhance its transdermal delivery [5].

Efinaconazole, a triazole antifungal agent, is primarily used in the treatment of dermatological conditions, particularly superficial mycoses. However, its poor water solubility limits its absorption through the skin, hindering its effectiveness in topical applications [6]. The main goal of this study was to develop a topical delivery system for efinaconazole that offers improved penetrability, rapid absorption, and high stability during storage [7]. The study utilized Response Surface Methodology, a chemometric technique, to assess the influence of chromatographic parameters on various quality indicators. The IV-optimal algorithm was used in the experimental design to create a proniosomal gel formulation of efinaconazole [8].

METHODS

Materials

Efinaconazole was kindly supplied by MSN Laboratories, Hyderabad. Sorbitan monopalmitate (Span40), sorbitan monostearate (Span60), soya lecithin, and cholesterol were purchased from SD Fine chemicals, Mumbai. Hetero Drugs Ltd., Hyderabad, provided the Transcutol HP, cyclomethicone, and hydroxypropyl methylcellulose grade K4M (viscosity approximately 4000 cp) as gift samples.

Formulation development

IV-optimal design for creating efinaconazole-loaded proniosomes

Preliminary experiments using a one-factor-at-a-time approach were first conducted to identify the key factors and the appropriate ranges within which the optimal conditions lie. The IV-optimal design was then implemented using Design-Expert® V8.0.1 software (Stat-Ease, Inc., Minneapolis, MN) to investigate the influence of four independent variables: cholesterol amount, surfactant amount, soya lecithin amount, and surfactant type on vesicle size and entrapment efficiency. The levels of these independent variables are provided in Table 1. The experiments were performed according to the design, and the resulting responses for the dependent variables are listed in Table 2. The response surfaces for the variables within the experimental domain were analyzed using Stat-Ease Design Expert® software V8.0.1. Following this, three additional confirmation experiments were conducted to validate the accuracy of the statistical experimental design.

Table 1: List of the independent and dependent variables used in the IV-optimal design

Independent variables			Levels		
Variable	**Name**	**Units**	**Low**	**Middle**	**High**
A	Amount of surfactant	mg	20	40	60
B	Amount of cholesterol	mg	150	300	450
C	Amount of soya lecithin	mg	50	75	100
D	Type of surfactant	--	Span 40		Span 60
Dependent variable			**Objective**		
Y1	Vesicle size	nm	Minimize		
Y2	Entrapment efficiency	%	Maximize		

Preparation of efinaconazole-loaded proniosomes

Efinaconazole proniosomes were prepared using the coacervation phase separation method [9]. The components, including Span 40, Span 60, cholesterol, and soy lecithin, were dissolved in 5 mL of ethanol and placed in a glass tube with a wide opening. To this solution, 200 mg of efinaconazole was added. The glass vial was then filled to the required level, sealed with a lid to reduce solvent evaporation, and gently heated in a water bath at 65±3°C to facilitate dissolution. The proniosomes were formed by introducing an aqueous phase (a 0.1% glycerol mixture) into the clear solution, followed by heating in the water bath and then cooling, which resulted in the formation of crystals. The prepared proniosomes were kept in opaque glass tubes for further characterization. To replenish the fluid levels in the system, 10 mL of phosphate buffer solution with a pH of 7.4 was subjected to sonication (Ultrasonic Bath Sonicator, Make - Frontline Electronics, Model - FS-2) at 37°C.

Evaluation of efinaconazole proniosomes

Vesicle size, polydispersity index, and zeta potential

The vesicle size of the proniosomes was analyzed using the Malvern Zetasizer Nano ZS (Malvern Instruments, UK). The freshly prepared hydrated niosomes were dispersed in double-distilled water for vesicle size characterization. Size measurements were performed in triplicate for each sample. The polydispersity index was also calculated to assess the homogeneity of the formulations. In addition, the zeta potential of the niosome formulations was measured to evaluate the stability of the formulations [10].

Entrapment efficiency

The entrapment efficiency was assessed by isolating the unentrapped drug. A 100 mg sample of proniosomes was hydrated with 10 mL of distilled water by manual shaking for 5 min. The percentage of entrapment efficiency of efinaconazole in the hydrated proniosomes was determined using the centrifugation method. The Eppendorf tube

Table 2: IV-optimum planning and observable outcomes

Run	Factor A Amount of surfactant	Factor B Amount of cholesterol	Factor C Amount of soya lecithin	Factor D Type of surfactant	Response Y1 vesicle size	Response Y2 entrapment efficiency
1	20	150	50	Span 40	213.72	52.82
2	20	150	50	Span 40	210.24	50.32
3	60	303	50	Span 40	216.84	56.56
4	40.232	450	50	Span 40	85.56	65.12
5	59.2	150	52.5	Span 40	342.76	40.35
6	20	307.5	73.48	Span 40	94.42	69.12
7	41	150	73.87883	Span 40	261.56	44.78
8	50.2	379.5	75	Span 40	146.82	58.86
9	60	150	79	Span 40	364.12	38.56
10	20	450	80	Span 40	58.24	69.12
11	20	150	100	Span 40	246.82	49.72
12	40.8	305.7478	100	Span 40	144.78	66.12
13	33.2	450	100	Span 40	82.78	66.24
14	60	450	100	Span 40	199.12	54.42
15	54.8	150	50	Span 60	182.54	51.56
16	54.8	150	50	Span 60	178.94	53.12
17	20	412.5	50	Span 60	46.92	81.82
18	20	412.5	50	Span 60	48.32	82.26
19	38.4	450	63.43612	Span 60	68.34	69.32
20	60	450	67.5	Span 60	150.46	61.12
21	40	300	75	Span 60	69.92	74.92
22	40	300	75	Span 60	70.12	73.34
23	20	150	82.5	Span 60	157.22	58.24
24	20	150	82.5	Span 60	156.82	57.72
25	49	390	99	Span 60	106.12	68.42
26	60	187.5	100	Span 60	216.78	56.12
27	60	187.5	100	Span 60	216.34	54.12
28	25.2	450	100	Span 60	86.54	76.34

containing the hydrated proniosomes was centrifuged at 14,000 rpm for 30 min at 4°C (Pico 21 centrifuge, Thermo Scientific HERAE US). The supernatant, containing the unentrapped drug, was collected and analyzed for free drug content by measuring its absorbance at λmax 262 nm using a UV-Vis spectrophotometer. The entrapment efficiency was calculated using the following formula:

$$Encapsulation\ efficiency\ (\%) = \frac{Amount\ of\ drug\ after\ filtration}{Total\ amount\ of\ drug\ in\ the\ sample} \times 100$$

Studies on drug-excipient compatibility

Drug-excipient compatibility studies were conducted to assess any potential interactions between the drug and the excipients. Fourier transform infrared (FTIR) spectroscopy was used to analyze the drug sample and its physical mixture with excipients. The spectra were recorded using the potassium bromide disc method on a Tensor 27 FTIR Spectrophotometer (Bruker Optics, Germany) in the range of 4000–600 cm^{-1}.

Differential scanning calorimetry (DSC) was performed on the drug sample and its physical mixture with excipients using a Perkin Elmer DSC/7 differential scanning calorimeter (Perkin-Elmer, CT-USA) equipped with a TAC 7/DX instrument controller. The instrument was calibrated with indium for melting point and heat of fusion measurements. A heating rate of 10°C/min was applied within the 30–400°C temperature range. Standard aluminum sample pans (Perkin-Elmer) were used, with an empty pan serving as the reference standard. The analyses were conducted in triplicate using 5 mg samples under a nitrogen purge [11,12].

Surface morphology

The morphological characterization of the proniosomal gel and the presence of its vesicular structure were confirmed by examining the surface morphology through optical microscopy. To characterize the surface of the proniosomes, a thin layer of the proniosomal gel was spread on a slide and viewed under an optical microscope. For optical microscopy, samples were prepared by hydrating 100 mg of proniosomal gel with phosphate buffer (pH 7.4). A drop of the dispersion was placed on a glass slide without a cover slip, and the process of niosome formation was observed using an optical microscope (LABOMED), with photographs captured by a digital camera [13].

Transmission electron microscopy (TEM)

The morphology of the prepared proniosomes was examined using TEM (JEM-2000 EXII; JEOL, Tokyo, Japan). A drop of diluted efinaconazole proniosomal suspension was placed on a film-coated copper grid and stained with a drop of 2% (w/v) aqueous phosphotungstic acid solution. The sample was then allowed to dry to enhance contrast. The samples were observed at a magnification of 72,000× using TEM [14].

In vitro drug release studies

In vitro release studies of hydrated efinaconazole proniosomal dispersions were performed using static Franz glass diffusion cells. The setup consists of two chambers: the donor and receptor chambers, separated by a cellulose membrane with a molecular weight cutoff range of 12,000–14,000 (Spectrum Medical Inc., Los Angeles, CA). The diffusion area available in this system was 1.7 cm^2. The dialysis membrane was hydrated in the receptor medium, which contained a phosphate buffer at pH 5.5 with 1% Tween 20, for 12 h before being placed in the Franz diffusion cell. A 2.5 mL solution of hydrated efinaconazole proniosomes was added to the donor chamber, while the receptor chamber was filled with 7.5 mL of receptor medium. The system was continuously stirred at 100 rpm and maintained at 37°C. Sampling was done at 1, 2, 3, 4, and 5 h. Samples were collected from the receptor chamber using a side-arm tube, and after each sample removal, an equal volume of receptor medium was added to maintain a constant volume. The efinaconazole content in the samples was determined by UV-Vis spectrophotometry at the maximum absorption wavelength (λmax) of 262 nm. The experiment was repeated in triplicate to ensure accuracy and reliability of the results [15].

Drug release kinetics

To understand the mode and mechanism of drug release, the data from the *in vitro* release study were analyzed using different kinetic models, including zero order, first order, Higuchi's, and Korsmeyer–Peppas models.

Stability studies

The stability study was conducted following the ICH guidelines. The proniosomal gel formulations were placed in tightly sealed glass vials and stored under two conditions: at room temperature (25±2°C) and in the freezer (4±1°C). After six months, the formulations were evaluated for vesicle size and entrapment efficiency [16,17].

Formulation of efinaconazole proniosomal gel

The candidate formulation was chosen based on the results of the IV-optimal design, which indicated an optimal vesicle size and maximum entrapment efficiency. The hydrogel was prepared by incorporating (hydroxypropyl methylcellulose [HPMC]) K4M (4000 cp viscosity) into the selected hydrated proniosomal formulation when continuously stirring at 800 rpm. In addition, Transcutol® HP was used as a penetration enhancer, along with cyclomethicone, which served as a wetting agent. The solution was stirred continuously until a uniform distribution was achieved. The dispersion was then neutralized with a triethanolamine solution. The composition of the hydrogel formulation is outlined in Table 3.

Characterization of efinaconazole proniosomal gel

Determination of pH and viscosity of proniosomal gel

The pH of all proniosomal gel formulations was measured using a digital pH meter (Elico India, Hyderabad) after being incorporated into the hydrogel. The viscosity of the drug's proniosomal gel was determined using a Brookfield Viscometer (LVDV E, Brookfield).

Study of ex vivo permeation

Ex vivo permeation studies were conducted using the skin of male Wistar rats [18]. The rat skin was placed between the donor and receptor compartments, with the stratum corneum facing upward in the diffusion cell. To maintain sink conditions, a 30% (v/v) ethanol solution in phosphate buffer (pH 7.4) was used in the receptor compartment. The temperature was maintained at 37±1°C. A proniosomal gel formulation equivalent to 10 mg of efinaconazole was applied to the rat skin. The contents of the receptor compartment were stirred with magnetic beads. Samples were collected at various time intervals and immediately replaced with fresh media. The drug content in the samples was analyzed using a UV-Vis spectrophotometer at 262 nm. The cumulative amount of drug permeated (Q) at different time intervals, along with parameters such as steady-state flux (Jss), permeability coefficient (Kp), and enhancement ratio (ER), were calculated using the following equations:

$$Steady\ state\ flux\ (Jss) = \frac{Amount\ of\ drug\ permeated\ (Q)}{Time \times Area\ of\ membrane}$$

Table 3: Composition of hydrogel formulation

S. No.	Component	Composition
1	Proniosomal formulation	Equivalent of 100 mg of drug
2	Transcutol® HP	2% w/w
3	Cyclomethicone	1% w/w
4	HPMC K4M	qty. sufficient to make 1 g

$$\text{Permeability coefficient}(K) = \frac{Flux(Jss)}{\begin{array}{l}Initial\ concentration\ of\\ drug\ in\ donor\ chamber\end{array}}$$

$$Enhancement\ ratio\ (ER) = \frac{Jss\ of\ \ proneosomess}{Jss\ of\ \ control}$$

The study was carried out in accordance with the Institutional Animal Ethical Committee (1447/PO/Re/S/11/COCSEA/106/A).

Skin irritation study of proniosomal gel

A 0.5 g application of proniosome gel was applied to the skin of three rats, covering an area of approximately 1" × 1" (2.54 cm × 2.54 cm) square. The animals were then returned to their cages. After 24 h of exposure, the proniosome gel was removed, and the test sites were wiped with tap water to remove any residual test article.

RESULTS AND DISCUSSION

Formulation development

In this study, efinaconazole proniosomes were formulated, optimized, and evaluated for their effectiveness in transdermal drug delivery to address the challenges associated with oral delivery. Initial experiments were conducted using various non-toxic, biocompatible non-ionic surfactants, such as Spans, in combination with cholesterol and soy lecithin. Typically, a cholesterol concentration of 20–30% is needed for optimal proniosome design. Given that Span 60 (53°C) and Span 40 (42°C) have high phase transition temperatures, they are capable of forming proniosomes both with and without cholesterol. Based on the preliminary experiment results, Span 40 and Span 60 were chosen as the most appropriate surfactants for preparing efinaconazole proniosomes (Fig. 1).

Optimization of variables

A total of 28 experiments were conducted, and the results are presented in Table 2. The parameters examined included the amount of surfactant (A), cholesterol (B), soy lecithin (C), and the type of surfactant (D). The data were analyzed using regression analysis with Design-Expert®, Version 8.0.1, Stat-Ease Inc., USA. To assess the significance of individual components, binary interactions, and quadratic terms on the responses, analysis of variance (ANOVA) was applied. A p=0.05 was considered to determine the significance of each factor. The executive summary of the design is shown in Fig. 2.

The vesicle size (Y1) for all trials ranged from 46.92 to 364.12 nm, and the entrapment efficiency varied between 38.56% and 82.26%. Mathematical relationships for the mentioned variables were derived using multiple linear regression analysis, as shown in Table 4. These equations describe the quantitative and interactive effects of independent factors on vesicle size (Y1) and entrapment efficiency (Y2). The coefficients of A, B, C, and D indicate the impact of these factors on the responses Y1 and Y2. Coefficients with multiple factors or higher-order terms represent interaction effects and quadratic relationships, respectively. A positive sign indicates a synergistic effect, while a negative sign denotes an antagonistic effect. A backward elimination procedure was used to fit the data to the quadratic model. Both polynomial equations were found to be statistically significant (p<0.01) based on ANOVA, as determined by the Design Expert software. The results of the multiple linear regression analysis for all models are provided in terms of R^2, adjusted R^2, predicted R^2, and coefficient of variation (Table 5). The high R^2 values suggest that the proposed models performed well. The adjusted R^2 values were consistent with the predicted R^2 values, confirming the models' ability to predict the response for new observations. The predicted R^2 values were not significantly lower than R^2, indicating that the model was not overfitting.

Figs. 3 and 4 show a reasonable agreement between the predicted and actual results. Each experimental value corresponds to its predicted value for all the responses. The results demonstrate that both models effectively identified the process and formulation variables involved in the preparation of efinaconazole proniosomes.

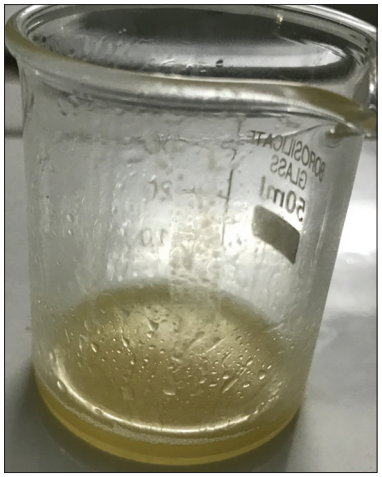

Fig. 1: Efinaconazole optimized proniosomes

The mathematical model for vesicle size (Y1) was found to be significant, with an F-value of 3405.66, indicating the model's significance. The chance of obtaining such a large "Model F-Value" due to noise is only 0.01%. A "Prob > F" value <0.0500 indicates that the model terms are significant. In this case, the significant model terms include A, B, C, D, AD, BC, BD, CD, A^2, and B^2. Terms with values >0.1000 are considered non-significant. The "Lack of Fit F-value" of 3.04 suggests that the lack of fit is not significant relative to the pure error, with a 9.3% chance that such a large "Lack of Fit F-value" could arise due to noise. A non-significant lack of fit is desirable because it indicates the model fits well. Statistical analysis showed that the quadratic model fits the data effectively, focusing on maximizing both the Adjusted R^2 and Predicted R^2. The "Pred R-Squared" value of 0.9987 is in good agreement with the "Adj R-Squared" value of 0.9993. The "Adeq Precision" ratio, which measures the signal-to-noise ratio, was 211.932, indicating an adequate signal since a ratio >4 is desirable. This model is suitable for navigating the design space. Table 6 demonstrates that the observed values closely match the predicted values.

The equation reveals that factors B and D have a negative effect on vesicle size, while factors A and C exert a significant positive effect. The individual impacts of factors A, B, and C on vesicle size are shown in the perturbation plot (Fig. 5). The plot clearly demonstrates that factors B and A have the most substantial effects on vesicle size, with factor C having a moderate influence. The categorical factor D indicates that Span 60 results in proniosomes with smaller particle sizes compared to Span 40. The relationship between the dependent and independent variables was further explored through 3D response surface plots and corresponding contour plots. Fig. 6 illustrates the interactive effect of A and C on vesicle size (Y1) at fixed levels of C and D. Fig. 7 shows the interactive effect of B and C on vesicle size (Y1) at fixed levels of A and D.

The entrapment efficiency of proniosomes ranged from 38.56% to 82.26%, as shown in Table 2. The polynomial equation for entrapment efficiency demonstrated a strong correlation coefficient (0.9890), and the Model F-value of 214.79 indicates that the model is significant. The probability of obtaining such a large "Model F-Value" due to noise is only 0.01%. Model terms with "Prob > F" values <0.0005 are considered significant. In this case, the significant terms include A, B, D, AB, A^2, B^2, and C^2, while terms with values greater than 0.1000 are non-significant. The "Lack of Fit F-value" of 1.86 suggests that the lack of fit is not significant relative to pure error, with a 22.87% chance that such a large "Lack of Fit F-value" could occur due to noise. A non-significant lack of fit is desirable, as it indicates a good model fit. The statistical

Design Summary

Study Type	Response Surface		**Runs**	28							
Design Type	IV-optimal	Coordin	**Blocks**	No Blocks							
Design Model	Quadratic		**Build Time (ms)**	4304.56							
Factor	**Name**	**Units**	**Type**	**Subtype**	**Minimum**	**Maximum**	**-1 Actual**	**+1 Actual**	**Mean**	**Std. Dev**	
A	Amount of cholesterol	mg	Numeric	Continuous	20.00	60.00	20.00	60.00	39.53	16.10	
B	Amount of surfactant	mg	Numeric	Continuous	150.00	450.00	150.00	450.00	290.56	126.09	
C	Amount of soyalecithin	mg	Numeric	Continuous	50.00	100.00	50.00	100.00	74.24	19.63	
D	Type of surfactent		Categoric	Nominal	Span 40	Span 60			**Levels:**	2	
Response	**Name**	**Units**	**Obs**	**Analysis**	**Minimum**	**Maximum**	**Mean**	**Std. Dev.**	**Ratio**	**Trans**	**Model**
Y1	Vesicle size	nm	28	Polynomial	46.92	364.12	157.97	84.9982	7.76044	None	RQuadratic
Y2	Entrapment efficiency	%	28	Polynomial	38.56	82.26	60.7332	11.549	2.1333	None	RQuadratic

Fig. 2: Summary of the IV-optimal design

Table 4: Regression equations for the responses – vesicle size and entrapment efficiency

Response	Regression equation
Y1	101.57+52.55 A−60.77 B+15.45 C−29.90D−1.36 AC−3.57 BC+33.85 A^2+45.37 B^2
Y2	68.07−6.91 A+8.03 B−0.52 C+4.40 D−1.67 AB−1.55 A^2−10.26 B^2+1.95 C^2

Table 5: Regression analysis

Dependent variable	R^2	Adjusted R^2	Predicted R^2	CV
Vesicle size (Y1)	0.9995	0.9992	0.9987	1.444
Entrapment efficiency (Y2)	0.9890	0.9844	0.9772	2.37

Table 6: Actual and predicted values of vesicle size (Y1)

Run order	Actual value	Predicted value	Residual
1	213.72	211.3364	2.383614
2	210.24	211.3364	−1.09639
3	216.84	219.0675	−2.22749
4	85.56	84.18898	1.371025
5	342.76	343.1122	−0.35225
6	94.42	93.92497	0.495027
7	261.56	264.0839	−2.5239
8	146.82	142.1246	4.69544
9	364.12	364.0651	0.0549
10	58.24	61.76731	−3.52731
11	246.82	246.2306	0.589369
12	144.78	143.3293	1.450698
13	82.78	83.02282	−0.24282
14	199.12	200.1899	−1.06992
15	182.54	180.2157	2.32425
16	178.94	180.2157	−1.27575
17	46.92	47.53911	−0.61911
18	48.32	47.53911	0.780894
19	68.34	70.23294	−1.89294
20	150.46	148.4719	1.988053
21	69.92	71.66884	−1.74884
22	70.12	71.66884	−1.54884
23	157.22	156.2923	0.927698
24	156.82	156.2923	0.527698
25	106.12	105.0602	1.059789
26	216.78	217.1813	−0.40128
27	216.34	217.1813	−0.84128
28	86.54	85.82035	0.719655

analysis showed that the quadratic model fits the data well, focusing on maximizing both Adjusted R^2 and Predicted R^2. The "Pred R-Squared" value of 0.9772 is in good agreement with the "Adj R-Squared" value of 0.9845. The "Adeq Precision" ratio, which measures the signal-to-noise ratio, is 53.034, indicating an adequate signal, as a ratio >4 is preferred. This model can be effectively used to navigate the design space, and

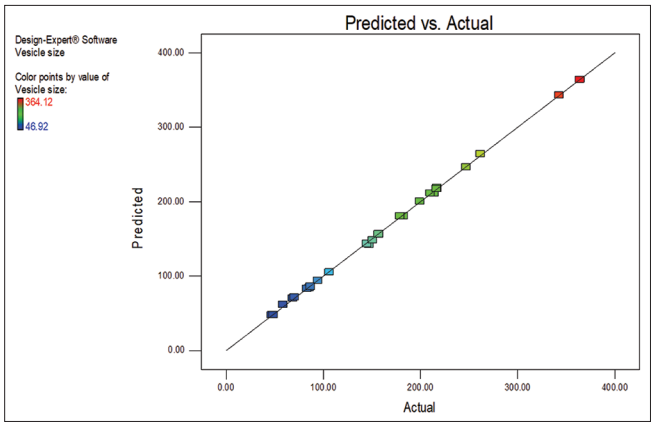

Fig. 3: Comparison between predicted and actual values of vesicle size

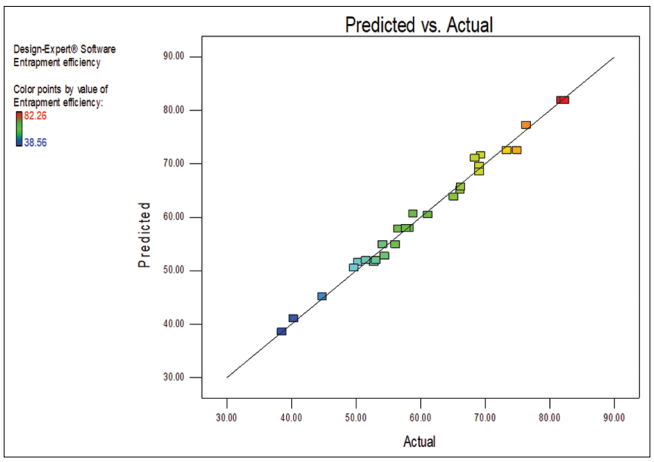

Fig. 4: Comparison between predicted and actual values of entrapment efficiency

Table 7 illustrates that the observed values align closely with the predicted values.

The equation clearly shows that factors A and C have a negative impact, while factors B and D significantly increase vesicle size. The individual effects of A, B, and C on vesicle size are illustrated in the perturbation plot (Fig. 8). The figure clearly demonstrates that B and A have the most considerable influence on entrapment efficiency, with C having a lesser effect. The categorical factor D indicates that Span 60 results in proniosomes with higher entrapment efficiency compared to Span 40. The relationship between the dependent and independent variables was further analyzed using 3D response surface plots and corresponding contour plots. Fig. 9 highlights the interactive effect of A and B on entrapment efficiency (Y2) at fixed levels of C and D.

Optimization and confirmation experiments

Derringer function static (D) calculated using the following equation.

$$D = (d_1(\hat{y}_i) \times d2(\hat{y}_2) \cdots \times dm(\hat{y}_m))^{\frac{1}{m}} = (\prod_{i=1}^{m} di(\hat{y}_i))^{\frac{1}{m}}$$

Both responses were converted into a desirability scale. Ymax and Ymin were defined as the objective function (D) for each response. Subsequently, each individual desirability function was combined using the geometric mean method through an extensive grid search and feasibility search within the domain to obtain a global desirability value via Design-Expert software. The resulting value of D was close to 1.0000, indicating the favorable impact of the combination of selected variables on the response. Constraints were applied to minimize vesicle size and maximize entrapment efficiency, which served as the goals for determining the optimal settings of independent variables.

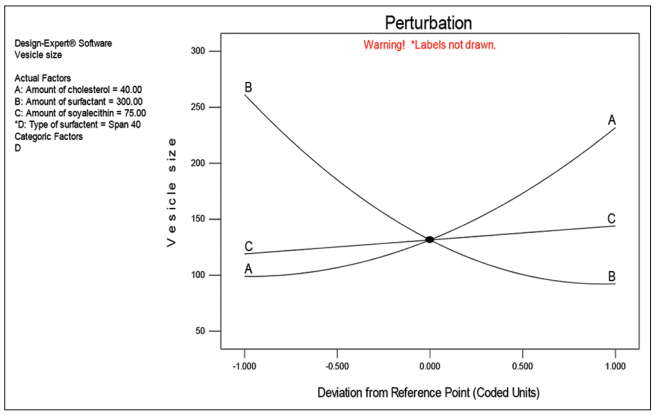

Fig. 5: Perturbation plot showing the effect of A, B and C on vesicle size

The factor levels and point prediction model are shown in Fig. 10. The three-dimensional response surface and contour plots represent the relationship between the fitted responses when examining the effects of two factors in each plot. The darkest zone on the graph indicates the highest desirability. These plots, showing the relationship between the response value on the Z-axis and two variables on the X- and Y-axes, are displayed in Fig. 11.

The optimized levels and predicted values for Y1 and Y2 are presented in Table 8. To validate these values, three batches of proniosomes were prepared based on the predicted levels of A, B, C, and D. The resulting Y1 and Y2 values closely matched the predicted ones, confirming the accuracy of the optimization procedure in forecasting the optimal parameters for the formulation of efinaconazole proniosomes. Following this, all three batches of efinaconazole proniosomes underwent further characterization.

Mean vesicle size, zeta potential, polydispersity index, and entrapment efficiency of optimized formulations

The vesicle size of the diluted proniosomes is presented in Table 9, ranging from 45.12±2.46 nm to 48.78±5.12 nm, with a unimodal particle size distribution, which is favorable for the transdermal delivery of efinaconazole (Fig. 12). Smaller vesicle sizes are beneficial for reducing irritation and enhancing the penetration of vesicles into the skin [19]. The polydispersity index for all formulations was low (<0.358), indicating good homogeneity of the preparation. All proniosome formulations exhibited negative charges, attributable to the negative charge of soya lecithin. The zeta potential values were high in all formulations (Table 9). The high zeta potential enhances repulsion between vesicles, preventing aggregation and flocculation (Fig. 13), thus electrically stabilizing the system.

Drug-excipients compatibility study

IR spectra and DSC data were examined for the pure drug, soy lecithin, cholesterol, and the physical mixtures of the drug with excipients. As shown in Fig. 14, there was no indication of any interaction between

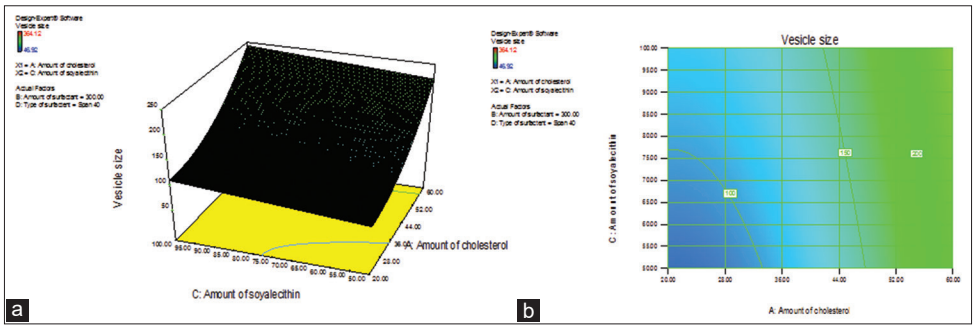

Fig. 6: (a) Response surface plot showing the interactive effect of A and C on the vesicle size (Y1) at fixed level of C and D (b) Contour plot showing the interactive effect of A and C on the vesicle size (Y1) at fixed level of C and D

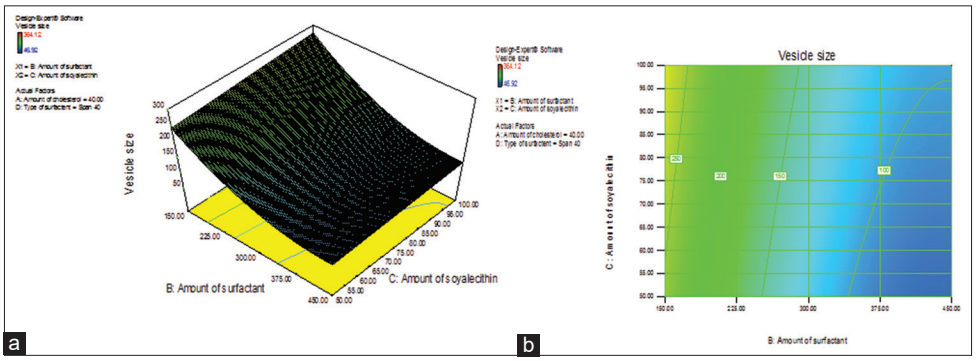

Fig. 7: (a) Response surface plot showing the interactive effect of B and C on the vesicle size (Y1) at fixed level of A and D (b) Contour plot showing the interactive effect of B and C on the vesicle size (Y1) at fixed level of A and D

efinaconazole and the excipients when compared to the IR spectra of the pure drug, as all functional group frequencies remained unchanged. The DSC findings, represented in Fig. 15, further indicate that there was no significant difference between the melting endotherms of the physical mixture and the pure drug [20]. The pronounced endotherm at 191.1°C confirmed the melting point of pure efinaconazole [22].

Table 7: Actual and predicted values of entrapment efficiency (Y2)

Run order	Actual value	Predicted value	Residual
1	52.82	51.55484	1.265162
2	50.32	51.55484	−1.23484
3	56.56	57.81975	−1.25975
4	65.12	63.83639	1.283614
5	40.35	40.98522	−0.63522
6	69.12	69.54156	−0.42156
7	44.78	45.14185	−0.36185
8	58.86	60.66772	−1.80772
9	38.56	38.55804	0.001957
10	69.12	68.46698	0.653022
11	49.72	50.5006	−0.7806
12	66.12	65.11994	1.000057
13	66.24	65.62511	0.614887
14	54.42	52.73717	1.68283
15	51.56	51.94766	−0.38766
16	53.12	51.94766	1.172344
17	81.82	81.84746	−0.02746
18	82.26	81.84746	0.412538
19	69.32	71.59536	−2.27536
20	61.12	60.44417	0.675832
21	74.92	72.48131	2.438693
22	73.34	72.48131	0.858693
23	58.24	57.89132	0.348676
24	57.72	57.89132	−0.17132
25	68.42	71.0288	−2.6088
26	56.12	54.90872	1.211279
27	54.12	54.90872	−0.78872
28	76.34	77.19873	−0.85873

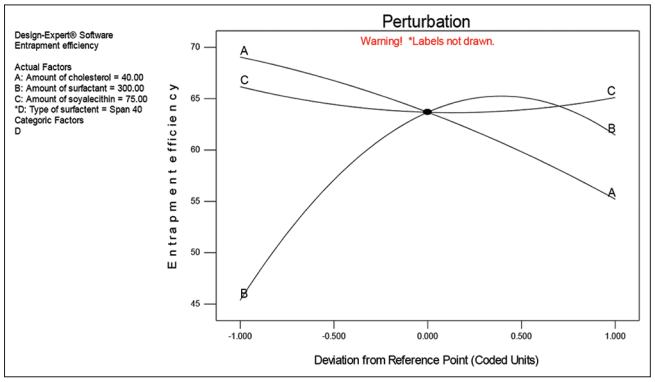

Fig. 8: Perturbation plot showing the effect of A, B and C on entrapment efficiency

Surface morphology

The efinaconazole-loaded proniosomal formulation, prepared using the optimal composition, exhibited lamellar structures under a compound microscope (Fig. 16). Upon hydration with saline solution, the formulation showed swelling of the bilayers and vesicles due to the interaction of water with the polar groups of the surfactant. The bilayers tended to form random spherical structures, leading to the formation of multilamellar and multivesicular structures. When shaken with the aqueous phase, complete hydration occurred, resulting in the formation of niosomes. Observation under an optical microscope revealed that the proniosomal gel rapidly and progressively converted to niosomes, almost completely within minutes.

TEM analysis

TEM analysis confirmed the presence of individual niosomes in a spherical shape, as shown in Fig. 17. These results provided clear evidence of niosome formation. Furthermore, the TEM findings were consistent with the particle size measurements obtained using dynamic light scattering, which further validated the niosomal structure.

In vitro drug release from proniosomes

From Fig. 18, it is evident that the cumulative release of efinaconazole from the control (efinaconazole in 30% PEG) was higher compared to the proniosomal formulation. This higher release from the control can be attributed to the fact that efinaconazole, being sufficiently lipophilic, partitions more readily in the PEG-based formulation, leading to a faster release. On the other hand, the proniosomal formulation showed a slower release of efinaconazole. This slower release can be attributed to the encapsulation of the drug within the proniosomes, which acts as a reservoir, gradually releasing the drug over time. In addition, the lower release rate observed with the proniosomal formula containing surfactant could be linked to the hydrophilic nature of the surfactant, which might influence the drug's release by forming a barrier around the drug particles, thus slowing down the release rate.

Drug release kinetics

The results clearly show that the zero-order model has a higher regression coefficient, indicating that the proniosomal formulation provides controlled drug release from its matrix. In contrast, the first-order model demonstrated less linearity, suggesting that it is not as suitable for describing the release. Further analysis of the dissolution data through mathematical models like Higuchi and Korsmeyer–Peppas helped elucidate the drug release mechanism. In the Korsmeyer–Peppas model, the release mechanism is determined by the value of n. A value of n <0.45 suggests Fickian diffusion, while a value between 0.45 and 0.89 indicates non-Fickian transport. A value of n < 0.45 indicates Fickian diffusion, while a value between 0.45 and 0.89 suggests non-Fickian transport. When n = 0.89, it corresponds to Case II (relaxational) transport. Values greater than 0.89 indicate super Case II transport. Therefore, the n-value of 0.63 obtained from the Korsmeyer–Peppas model signifies super Case II transport, as shown in Table 10.

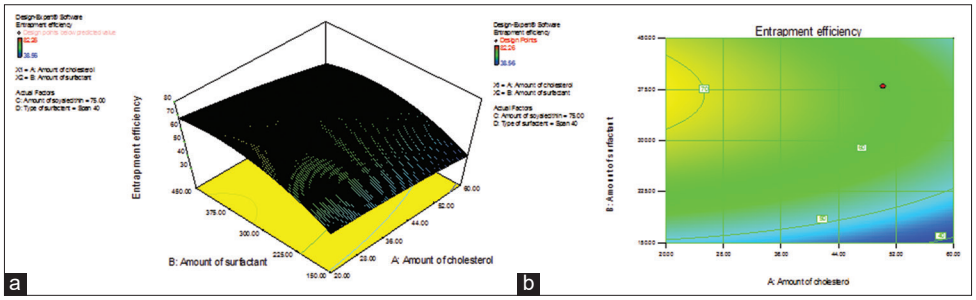

Fig. 9: (a) Response surface plot showing the interactive effect of A and B on the entrapment efficiency (Y2) at fixed level of C and D (b) Contour plot showing the interactive effect of A and B on the entrapment efficiency (Y2) at fixed level of C and D

Table 8: Optimized values obtained by the constraints applies on Y1 and Y2

Independent variable	Nominal values	Predicted values		Observed values		
		Particle size (Y1)	Entrapment efficiency (Y2)	Batch	Particle size (Y1)	Entrapment efficiency (Y2)
Amount of surfactant (A)	20.61	42.41	82.30	1	46.34	79.12
				2	48.78	81.82
Amount of cholesterol (B)	387.34			3	45.12	80.56
Amount of soya lecithin (C)	50.32					
Type of surfactant	Span 60					

Table 9: Optimized formulations' average vesicle size, polydispesity index, entrapment effectiveness, and zeta potential

Batch	MVS±SD (nm)	PDI	ZP±SD (mV)	% EE±SD
1	46.34±5.12	0.284	-28.3±1.2	79.12±3.12
2	48.78±4.36	0.312	-25.5±2.3	81.82±4.37
3	45.12±2.46	0.358	-23.5±3.1	80.56±4.18

MVS: Mean vesicle size, PDI: Polydispersity index, ZP: Zeta potential, EE: Entrapment efficiency, SD: Standard deviation. All the values were expressed in (n=3) mean±SD; ($p<0.05$)

Table 10: Release kinetics of efinaconazole proniosomal formulation

Formulation code	Zero order		First order		Higuchi		Korsmeyer-Peppas	
	R^2	n	R^2	n	R^2	n	R^2	n
F1	0.9989	4.064	0.6587	−0.0676	0.9101	19.4911	0.8037	63.57

Factor	Name	Level	Low Level	High Level	Std. Dev.	Coding
A	Amount of cholesterol	20.61	20.00	60.00	0.000	Actual
B	Amount of surfactant	387.34	150.00	450.00	0.000	Actual
C	Amount of soyalecithin	50.32	50.00	100.00	0.000	Actual
D	Type of surfactent	Span 60	Span 40	Span 60	N/A	Actual

Response	Prediction	SE Mean	95% CI low	95% CI high	SE Pred	95% PI low	95% PI high	90% of Population 95% TI low	95% TI high
Vesicle size	42.4174	1.44	39.36	45.48	2.70	36.69	48.14	34.58	50.26
Entrapment efi	82.3074	0.80	80.64	83.97	1.64	78.86	85.75	77.69	86.93

Fig. 10: Optimum level of factors and point prediction

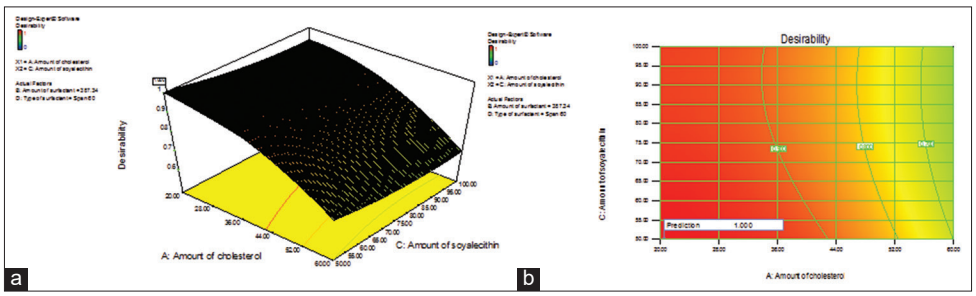

Fig. 11: The 3-dimensional response surface plot and contour plots showing the relationship between a response value on the Z-axis and two variables on the X- and Y-axes

Stability study

Stability testing is conducted to assess how the quality of a drug substance or product changes over time due to various environmental factors such as heat, humidity, and light. The results showed no significant difference in the entrapment efficiency and particle size of the optimized formulation when stored at room temperature and under refrigeration ($p>0.05$; Table 11).

Characterization of efinaconazole proniosomal gel

Determination of pH and viscosity of proniosomal gel

The pH of the final efinaconazole hydrogel formulation was initially 7.16, necessitating the use of triethanolamine to adjust it to a pH of 5.6. The viscosity of the final formulation was measured at 1580.24 cps, which falls within the acceptable range. The prepared gel is shown in Fig. 19.

Ex vivo permeation studies

By comparing the release rate (flux) of efinaconazole across the membrane and excised skin (Table 12), insights can be gained into the skin's natural defense mechanisms [23-25]. It is well established that proniosomes hydrate upon contact with skin moisture, forming niosomes, which can alter drug transport across the skin. The adsorption and fusion of niosomes onto the skin surface facilitate

Table 11: Vesicle size and entrapment efficiency of efinaconazole proniosomes after 180 days of storage at refrigerated and room temperature

Temperature (°C)	Particle size (nm)			Entrapment efficiency (%)			Release data (% CDR)					
	0 months	3 months	6 months	0 months	3 months	6 months	0 months		3 months		6 months	
							2 h	4 h	2 h	4 h	2 h	4 h
4±1°C	46.34±5.12	50.34±4.12	51.68±2.66	79.12±3.12	80.12±3.82	78.56±4.12	9.73±1.26	17.12±0.86	8.98±0.89	18.22±1.28	11.34±2.65	19.34±2.26
25±2°C	46.34±5.12	48.38±3.72	63.42±3.12	79.12±3.12	79.54±2.38	73.12±5.36	9.73±1.26	17.12±0.86	9.12±3.28	17.86±2.12	12.12±3.42	21.34±1.74

All the values were expressed in (n=3) mean±SD ($p<0.05$)

Table 12: Flux of efinaconazole from proniosomal gel

Formulation	Flux (µg cm^{-2} h^{-1})	
	Egg membrane	Rat skin
F1	44.182±3.34	186.72±9.734
Control	276.54±5.14	62.58±4.34

All the values were expressed in (n=3) mean±SD

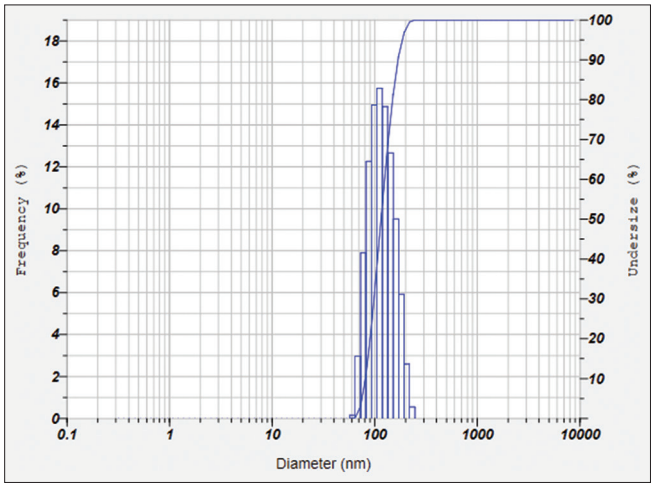

Fig. 12: A graphical representation of vesicle size of optimized formulation

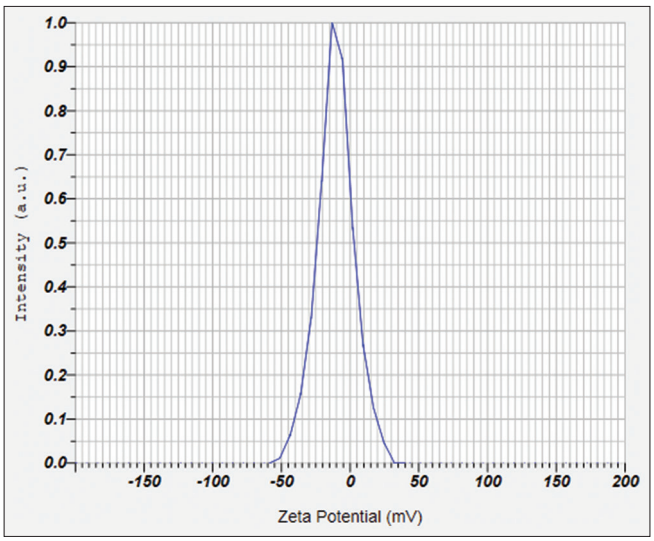

Fig. 13: A graphical representation of zeta potential of optimized formulation

drug permeation by modifying the barrier properties of the stratum corneum. Non-ionic surfactants, acting as penetration enhancers, disrupt the tightly packed lipids in the extracellular spaces of the stratum corneum. Significant differences in the release rate (flux) of efinaconazole between the membrane and excised skin (Table 12) highlight the skin's barrier properties. The interaction between the skin and proniosome components likely accounts for these differences, with the association and fusion of niosomes with the skin surface resulting in higher flux due to the direct transfer of the drug from the vesicles [26].

Skin irritation studies

Irritation studies were performed on male Wistar rats (n=3), with formalin used as the standard irritant. The rats were assessed for

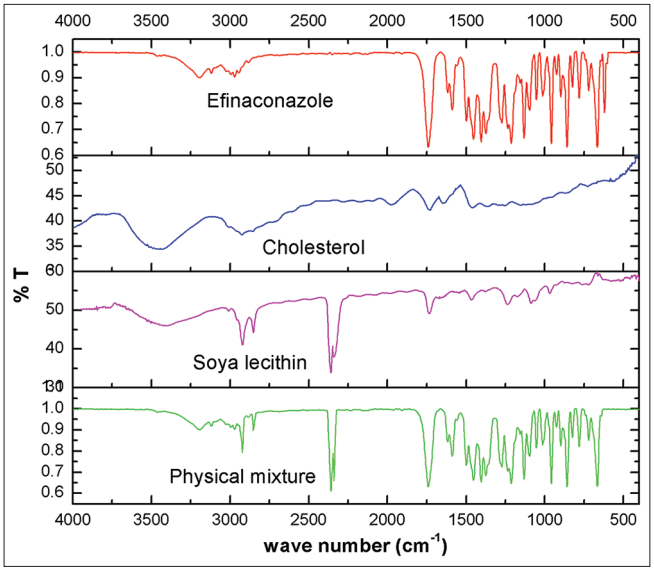

Fig. 14: Fourier Transform Infrared spectra of efinaconazole, cholesterol, soya lecithin and physical mixture

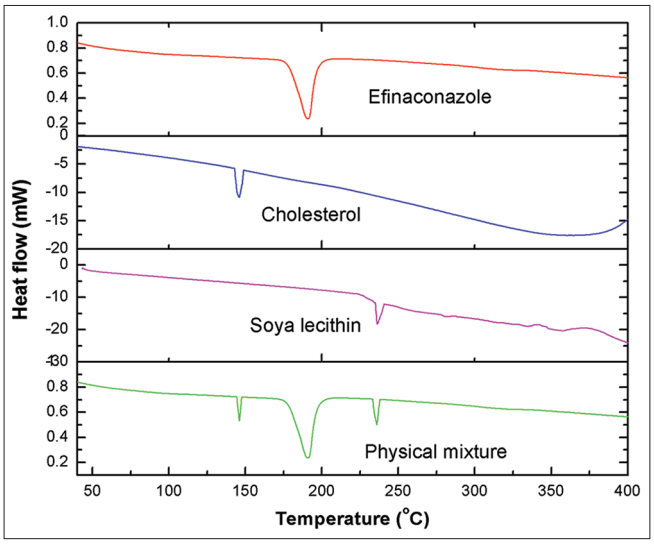

Fig. 15: Differential scanning calorimetry thermogram of efinaconazole, cholesterol, soya lecithin and physical mixture

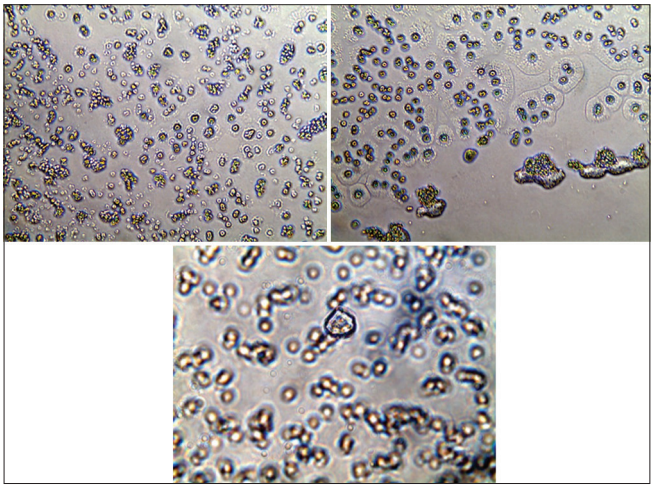

Fig. 16: Optical microscopy images of niosomes formed upon hydration of proniosomal formulation at ×1000 magnification

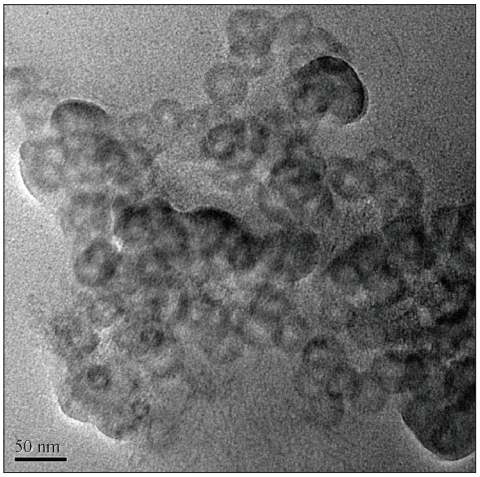

Fig. 17: TEM image of efinaconazole niosomes

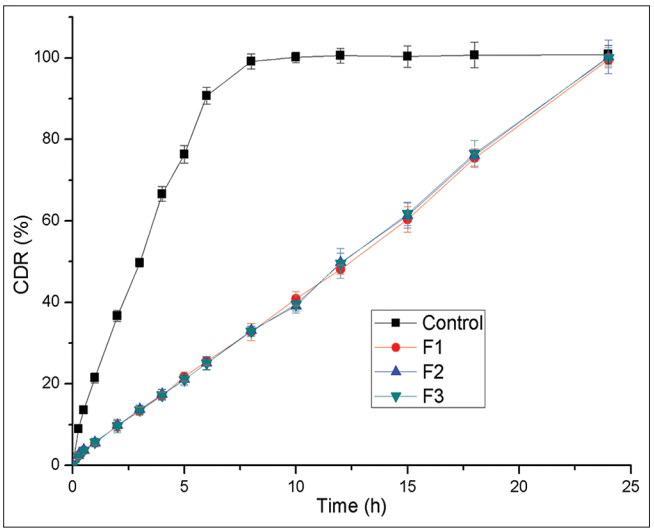

Fig. 18: *In-vitro* release of efinaconazole from proniosomes. All the values were expressed in (n=3) mean±SD

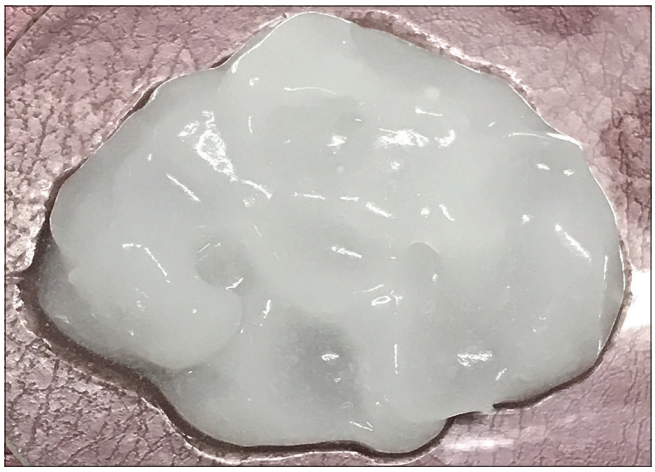

Fig. 19: Efinaconazole proniosomal gel

erythema and edema according to a defined scale [27-29]. The results showed significantly lower incidences of erythema and edema (0.32±0.098; $p<0.05$) in rats treated with the proniosomal gel formulations compared to those treated with formalin. This suggests that the formulations were non-irritant and safe [30,31].

CONCLUSION

This study highlights the application of IV-optimal design, regression analysis, and contour plots to optimize formulation variables in the preparation of efinaconazole proniosomes using the coacervation phase separation method. The optimized proniosomal batch was utilized to prepare an efinaconazole-based proniosomal hydrogel by incorporating hydrated niosomes into an HPMC matrix. The improved skin permeation over an extended period may lead to enhanced efficacy and better patient compliance. Overall, the study suggests that the niosomal gel formulation containing efinaconazole could offer therapeutic benefits superior to those of conventional formulations.

AUTHORS CONTRIBUTION

SV conducted the research, executed the experiments, and wrote the manuscript. RGV was responsible for the work plan, review, and revisions. All authors have agreed to the submission and publication of the manuscript and have read and approved the final version.

CONFLICT OF INTEREST

None.

FUNDING

This research received no external funding.

REFERENCES

1. Prausnitz MR, Langer R. Transdermal drug delivery. Nat Biotechnol. 2008 Nov;26(11):1261-8. doi: 10.1038/nbt.1504
2. Patel D, Chaudhary SA, Parmar B, Bhura N. Transdermal drug delivery system: A review. Pharma Innov J. 2012 Jan;1(4, Part A):66.
3. Tavano L, Gentile L, Oliviero Rossi C, Muzzalupo R. Novel gel-niosomes formulations as multicomponent systems for transdermal drug delivery. Colloids Surf B Biointerfaces. 2013 Apr;110:281-8. doi: 10.1016/j.colsurfb.2013.04.017
4. Khatoon M, Shah KU, Din FU, Shah SU, Rehman AU, Dilawar N, *et al*. Proniosomes derived niosomes: Recent advancements in drug delivery and targeting. Drug Deliv. 2017 Jan;24(Sup 1):56-69. doi: 10.1080/10717544.2017.1384520
5. Ajrin M, Anjum F. Proniosome: A promising approach for vesicular drug delivery. Turk J Pharm Sci. 2022 Apr;19(4):462-75. doi: 10.4274/tjps.galenos.2021.53533
6. Taghipour S, Kiasat N, Shafiei S, Halvaeezadeh M, Rezaei-Matehkolaei A, Zarei Mahmoudabadi A. Luliconazole, a new antifungal against *Candida* species isolated from different sources. J Mycol Med. 2018 Feb;28(2):374-8. doi: 10.1016/j.mycmed.2017.11.004
7. Kaur M, Singh K, Jain SK. Luliconazole vesicular based gel formulations for its enhanced topical delivery. J Liposome Res. 2020 Apr;30(4):388-406. doi: 10.1080/08982104.2019.1682602
8. Myers RH, Montgomery DC, Anderson-Cook CM. Response Surface Methodology: Process and Product Optimization Using Designed Experiments. Hoboken, NJ: John Wiley and Sons; 2016.
9. Vora B, Khopade AJ, Jain NK. Proniosome based transdermal delivery of levonorgestrel for effective contraception. J Control Release. 1998 Feb;54(2):149-65. doi: 10.1016/s0168-3659(97)00100-4
10. Ibrahim MM, Sammour OA, Hammad MA, Megrab NA. *In vitro* evaluation of proniosomes as a drug carrier for flurbiprofen. AAPS PharmSciTech. 2008 Mar;9(3):782-90. doi: 10.1208/s12249-008-9114-0
11. Ammar HO, Mohamed MI, Tadros MI, Fouly AA. Transdermal delivery of ondansetron hydrochloride via bilosomal systems: *In vitro*, *ex vivo*, and *in vivo* characterization studies. AAPS PharmSciTech. 2018 May;19(5):2276-87. doi: 10.1208/s12249-018-1019-y
12. Kurakula M, Ahmed OA, Fahmy UA, Ahmed TA. Solid lipid nanoparticles for transdermal delivery of avanafil: Optimization, formulation, *in-vitro* and *ex-vivo* studies. J Liposome Res. 2016 Apr;26(4):288-96. doi: 10.3109/08982104.2015.1117490
13. Akhtar M, Imam SS, Afroz Ahmad M, Najmi AK, Mujeeb M, Aqil M. Neuroprotective study of *Nigella sativa*-loaded oral provesicular lipid formulation: *In vitro* and *ex vivo* study. Drug Deliv. 2014 Jun;21(6):487-94. doi: 10.3109/10717544.2014.886640
14. Shamsheer Ahmad S, Sabareesh M, Khan PR, Sai Krishna P, Sudheer B. Formulation and evaluation of lisinopril dihydrate transdermal proniosomal gels. J Appl Pharm Sci. 2011 Aug;1(8):181-5.
15. Imam SS, Aqil M, Akhtar M, Sultana Y, Ali A. Formulation by design-based proniosome for accentuated transdermal delivery of risperidone: *In vitro* characterization and *in vivo* pharmacokinetic study. Drug Deliv. 2015 Aug;22(8):1059-70. doi: 10.3109/10717544.2013.870260
16. Rahman SA, Abdelmalak NS, Badawi A, Elbayoumy T, Sabry N, El Ramly A. Formulation of tretinoin-loaded topical proniosomes for treatment of acne: *In-vitro* characterization, skin irritation test and comparative clinical study. Drug Deliv. 2015 Jun;22(6):731-9. doi: 10.3109/10717544.2014.896428
17. Ashar F, Hani U, Osmani RA, Kazim SM, Selvamuthukumar S. Preparation and optimization of ibrutinib-loaded nanoliposomes using response surface methodology. Polymers (Basel). 2022 Jan;14(18):3886. doi: 10.3390/polym14183886
18. Derringer G, Suich R. Simultaneous optimization of several response variables. J Qual Technol. 1980 Apr;12(4):214-9. doi: 10.1080/00224065.1980.11980968
19. Kumar M, Shanthi N, Mahato AK, Soni S, Rajnikanth PS. Preparation of luliconazole nanocrystals loaded hydrogel for improvement of dissolution and antifungal activity. Heliyon. 2019 May;5(5):e01688. doi: 10.1016/j.heliyon.2019.e01688
20. Mokhtar M, Sammour OA, Hammad MA, Megrab NA. Effect of some formulation parameters on flurbiprofen encapsulation and release rates of niosomes prepared from proniosomes. Int J Pharm. 2008 Feb;361(1-2):104-11. doi: 10.1016/j.ijpharm.2008.05.031
21. Yousuf M, Ahmad M, Usman M, Ali I. Ketotifen fumarate and salbutamol sulphate combined transdermal patch formulations: *In vitro* release and *ex vivo* permeation studies. Indian J Pharm Sci. 2013 May;75(5):569-77.
22. Abdelbary GA, Amin MM, Zakaria MY. Ocular ketoconazole-loaded proniosomal gels: Formulation, *ex vivo* corneal permeation and *in vivo* studies. Drug Deliv. 2017 Jan;24(1):309-19. doi: 10.1080/10717544.2016.1247928
23. Chauhan SB, Naved T, Parvez N. Formulation development and evaluation of proniosomal gel of ethinylestradiol and levonorgestrel for antifertility treatment. Asian J Pharm Clin Res. 2019 Jan;12(1):364-8.
24. Parvez Baig R, Wais M. Formulation and development of proniosomal gel for topical delivery of amphotericin B. Int J Pharm Pharm Sci. 2022 Jan;14(1):37-49.
25. Jalajakshi MN, Chandrakala V, Srinivasan S. An overview: Recent development in transdermal drug delivery. Int J Pharm Pharm Sci. 2022 Oct;14(10):1-9.
26. Prashar D, Kumar V, Jasra K. Combination effect of luliconazole and clobetasol for treatment of skin ailments. Int J Curr Pharm Res. 2022 Mar;14(2):36-40.
27. Madhavi N, Sudhakar B, Sravani U. Development and evaluation of itraconazole solid dispersion gel cutaneous delivery. Int J App Pharm. 2023 Jul;15(6):334-41.
28. Narwade VL, Singh N. Preparation, optimization, compatibility study of captopril proniosome, and *in-vitro*, *in-vivo* evaluation of release study. Int J Pharm Qual Assur. 2023 Feb;14(2):323-9. doi: 10.25258/ijpqa.14.2.14
29. Reddy KS, Bhikshapathi D. Design and optimization of DPC-crosslinked HPβCD nanosponges for entrectinib oral delivery: Formulation, characterization, and pharmacokinetic studies. Futur J Pharm Sci. 2024 Mar;10:101. doi: 10.1186/s43094-024-00569-5
30. Viswaja M, Bhikshapathi DV, Palanati M, Babu AK, Goje A. Formulation and evaluation of ibrutinib nanosponges incorporated tablet. Int J Appl Pharm. 2023 Feb;15(2):92-7. doi: 10.22159/ijap.2023v15i2.46813
31. Viswaja M, Bhikshapathi DV, Sadasivam RK, Goje A, Cheruku S. Formulation and evaluation of liquid based supersaturable selfnanoemulsifying drug delivery system of manidipine. Int J Pharm Sci Drug Res. 2023 Jan-Mar;15(1):80-7.